Latin American Journal of Solids and Structures
www.lajss.org

Control of a Support Excitation Smart Beam Subjected to a Follower Force with Piezoelectric Sensors/Actuators

Abstract

In this paper, an active control is used to suppress the flutter vibration of a support excitation beam subjected to a follower force, using piezoelectric sensors/actuators. The beam is fixed to a motion support from one end and the other end is subjected to a follower force. The governing equations of motion are derived based on the generalized function theory and Lagrange-Rayleigh-Ritz technique, considering the Euler-Bernoulli beam theory. A robust Lyapunov based control scheme is applied to the system to suppress the induced flutter vibrations of the beam. The mathematical modeling of the beam with control algorithm is derived. Finally the system is simulated and the effects of the type of excitation, the magnitude of the follower force, instrument disturbances, and parameter uncertainties are studied. The simulation results show the applicability and robustness of the controller algorithm.

Keywords

Robust Lyapunov based control; Smart beam; Support excitation; Piezoelectric layers; Follower force

Mohammad Azadi [a]
Emad Azadi [b]
S. Ahmad Fazelzadeh [b]

[a] Department of Mechanical Engineering, Marvdasht Branch, Islamic Azad University, Marvdasht, I.R. Iran.
E-mail: mazadi@shirazu.ac.ir
[b] School of Mechanical Engineering, Shiraz University, Shiraz, I.R. Iran

http://dx.doi.org/10.1590/1679-78252047

Received 13.04.2015
In Revised Form 24.06.2015
Accepted 02.07.2015
Available online 07.07.2015

1 INTRODUCTION

Vibration suppression of a cantilever beam with support motion has been the subject of much attraction in recent years. Jalili et al. (2002) have presented a non model-based controller for a flexible cantilever beam with PZT patch actuator attachment and subjected to a moving base. They used the linear formulations to drive the equation of motion. Foutsitzi et al. (2003) studied vibration control of a beam with bonded piezoelectric sensors and actuators. They derived the equation of motion for the beam structure by using the Hamilton's principle. They also designed a H_2 robust controller and showed that the vibration can be significantly suppressed by the proposed controller. Sun et al. (2004) described an approach for the use of smart materials, specifically, piezoelectric materials (PZT), in control of a single-link flexible manipulator. Lin and Nien (2005) investigated

modeling and vibration control of a composed cantilever beam using piezoelectric damping-model actuators/sensors. Lin and Liu (2006) presented a novel resonant fuzzy logic controller (FLC) to minimize cantilever beam vibration using collocated piezoelectric actuator/sensor pairs. An active control scheme was used to restrain vibration of a cantilever beam system by Xinke and Haimin (2007). Mahmoodi et al. (2008) studied the nonlinear vibration analysis of a directly excited cantilever beam modeled as an inextensible viscoelastic Euler-Bernoulli beam. Santillan et al. (2008) investigated Large-amplitude in-plane beam vibration using numerical simulations and a perturbation analysis applied to the dynamic elastic model. Alhazza et al. (2009) developed a simple multimode delayed-acceleration feedback controller to mitigate the vibrations of a flexible cantilever beam using a single sensor and a single piezoelectric actuator. Ji et al. (2010) studied a switch control strategy based on an energy threshold for vibration control of a beam. Enhancement of the buckling and flutter capacities of a column by the attachment of an arbitrary lumped mass is studied by Fazelzadeh et al. (2010). An analysis of three active-passive damping design configurations applied to a cantilever beam was presented by Trindade(2011). He studied two design configurations based on the extension mode of piezoelectric actuators combined with viscoelastic constrained layer damping treatments and one design configuration with shear piezoelectric actuators embedded in a sandwich beam with viscoelastic core. Kucuk et al. (2011) applied an optimal control to suppress the vibrations of an Euler-Bernoulli beam with piezoelectric layers as actuators. An H_∞ method for the vibration control of an iron cantilever beam with axial velocity using the noncontact force by permanent magnets was proposed by Wang et al. (2011). They derived the governing equations of motion using D'Alembert's principle and then updated them by experiments. Kucuk et al. (2012) presented an active vibration control of the transverse modes, which is implemented by discrete sets of piezoelectric actuators which apply the optimal forces, in a flexible elastic system. They made use of a combination of Galerkin and variational approaches to determine the control forces in the time domain explicitly in terms of coupled amplitudes and velocities. Dynamic stability analysis and vibration control of a rotating elastic beam connected with an end mass driven by a direct current (DC) motor has been studied by Kuo et al. (2013). Fazelzadeh and Kazemi-Lari (2013) studied the stability of a cantilever beam resting on an elastic foundation under the action of a uniformly distributed tangential load. Prokic et al. (2014) presented a numerical method for solution of the free vibration of beams governed by a set of second order ordinary differential equations. Sinir et al. (2014) studied the exact solution of buckling and vibration response of post-buckling configurations of beams with non-classical boundary conditions. Azadi et al. (2014) applied an active control to suppress the vibration of a FGM beam. Thevibration of a gold nano-beam which has been induced by laser pulse heating is investigated by Youssef et al. (2015).

In this study, a cantilever beam with attached piezoelectric layers is considered. The support of the beam can move and excite the lateral vibration in it and a follower force is applied to the end of the beam. Lagrange Reilly-Ritz method is used to obtain the governing equation of motion. A robust controller is used to damp the lateral vibration of the beam. Finally, the system is simulated and the simulation results show the high performance of the controller.

By a thorough look at the literature, it is understood that the study of the suppression of the flutter vibration of a support excitation beam under follower force is important and requires attention. In spite of the wide researches in the area of the control vibration of the beams, there has been

no attempt to tackle the problem described in the present paper. Applying an active control to suppress the flutter vibration of a support excitation beam under follower force, using piezoelectric sensors/actuators, and analyzing the stability of the beam in different conditions is the main contribution of the present paper.

2 SYSTEM DYNAMICS

Figure 1 shows the schematic view of the system. This system consists of a support motion cantilever beam subjected to a follower force. The piezoelectric layers are attached on both side of the beam as sensors/actuators.

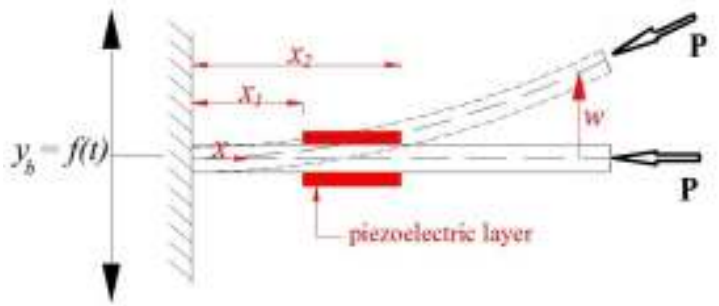

Figure 1: Schematic view of the smart beam.

The system considered as a cantilever beam with width b, thickness h, length l, density ρ_b, and Young's modulus E to which the piezoelectric layers are attached. Each piezoelectric layer has thickness h_p, density ρ_p, Young's modulus E_p and equivalent piezoelectric coefficient e_{31}. $w(x)$ represents the lateral deflection of the beam. Each pair of piezoelectric layers is attached on opposite sides of the beam from x_{1_n} to x_{2_n} (n=1, 2. . . N). Herein N is the number of piezoelectric layers.

The Lagrange's equations are used to determine the dynamical equations of the system.

$$\frac{\partial T}{\partial q} - \frac{d}{dt}\left(\frac{\partial T}{\partial \dot{q}}\right) + \frac{\partial U}{\partial q} = Q \tag{1}$$

herein $T = T_b + T_p$, $U = U_b + U_p$, and Q are the kinetic energy, potential energy, and generalized forces, respectively. The subscripts b, and p stand for beam, and piezoelectric layers, respectively. q is the generalized coordinates.

The displacement of each element of the beam can be determined as follows

$$y(x,t) = w(x,t) + y_b(t) \tag{2}$$

where $y_b(t)$ is the movement of the beam support.

Each term of the system kinetic energy is determined as:

$$T_b = \frac{1}{2}\int_0^l \rho_b \dot{y}^2(x,t)dx = \frac{1}{2}\int_0^l \rho_b [\dot{w}(x,t) + \dot{y}_b(t)]^2 dx$$
$$T_p = \frac{1}{2}\sum \int_{x1_n}^{x2_n} \rho_{p_n} \dot{y}^2(x,t)dx = \frac{1}{2}\sum_n \int_{x1_n}^{x2_n} \rho_{p_n} [\dot{w}(x,t) + \dot{y}_b(t)]^2 dx \quad (3)$$

The potential energy of the system is obtained as

$$U_b = \frac{1}{2}\int_{beam} Ez^2 (\frac{\partial^2 w}{\partial x^2})^2 dV + \frac{1}{2}\int_0^L P(\frac{\partial w}{\partial x})^2 dx$$
$$U_p = \frac{1}{2}\sum_{n=1}^{N} \int_{PZT_n} E_{p_n} z^2 (\frac{\partial^2 w}{\partial x^2})^2 dV + \frac{1}{2}\sum_{n=1}^{N} \int_{PZT_n} e_{31n} \frac{v_n}{h_p} (z\frac{d^2 w}{dx^2}) dV + \frac{1}{2}\sum_{n=1}^{N} \int_{PZT_n} E_{z_n} d_n dV \quad (4)$$

where dV is a volume differential element of the beam. According to the second part of Eq. (4), the potential energy of the piezoelectric layers is divided into elastic and electric parts. The subscript p_n represents the nth piezoelectric layers and $E_{z_n} = v_n / h_{p_n}$ $(n = 1...N)$ is the electric field in the nth piezoelectric layer. d_n is the electric displacement for the nth patch. The last term in piezoelectric potential energy equation is the electric energy stored in the piezoelectric material. The electric displacement is

$$d_n = \varepsilon_{p_n} \frac{v_n}{h_{p_n}} \quad (5)$$

where ε_{p_n} is the dielectric constant of the piezoelectric material which forms the nth patch.

The non-conservative work which is done by the follower force is

$$W = P\frac{\partial w(L,t)}{\partial x} w(L,t) \quad (6)$$

By knowing that $\delta W = Q^T \delta q$, the vector of generalized forces can be easily determined from Equation (6).

Due to the intricacy of the governing equations, the solution may be achieved by an approximate solution procedure. To this end, w can be represented by a series of trial shape functions, s_i, satisfying the boundary conditions, which each of them is multiplied by a time dependent generalized coordinate, q_i, that is,

$$w(x,t) = \sum_i s_i(x) q_i(t) = s^T q \quad (7)$$

where s and q are the vectors of assumed mode shapes and generalized coordinates of the beam, respectively.

By substituting equations (7) into equations (3-6), applying the Rayleigh-Ritz procedure on the governing equations the following set of ordinary differential equations is obtained:

$$(M_b + M_p)\ddot{q} + (K_b + K_p + K_W)q = -K_{p_{elastelect_a}} v_a - \ddot{y}_b \int_0^l \rho_b s dx - \ddot{y}_b \sum_N^{x_{2_n}} \int_{x_{1_n}} \rho_{p_n} s dx$$
$$v_s = K^{-1}_{p_{elect}} K^T_{p_{elastelect_s}} q \tag{8}$$

where M_b, and M_p are the beam, and piezoelectric inertial matrices. K_b, K_p, and K_W are the beam, and piezoelectric stiffness matrices, and the stiffness effects of the follower force, respectively. These parameters are defined as

$$M_b = \int_0^L \int_{\frac{-h_f}{2}}^{\frac{h_f}{2}} b\rho_b(z) s(x) s^T(x) dz dx$$
$$M_p = \sum_{n=1}^{N} \int_{x_{1_n}}^{x_{2_n}} \rho_{p_n} b_{p_n} h_{p_n} s(x) s^T(x) dx \tag{9}$$

and

$$K_b = \int_0^L P \frac{\partial s(x)}{\partial x} \frac{\partial s^T(x)}{\partial x} dx + \int_0^L \int_{\frac{-h}{2}}^{\frac{h}{2}} b z^2 E \frac{\partial^2 s(x)}{\partial x^2} \frac{\partial^2 s^T(x)}{\partial x^2} dz dx$$
$$K_p = \sum_{n=1}^{N} \iiint_{PZT_n} E_{p_n} z^2 \frac{\partial^2 s(x)}{\partial x^2} \frac{\partial^2 s^T(x)}{\partial x^2} d\mathrm{v} \tag{10}$$
$$K_w = -Ps(L) \frac{\partial s^T(x)}{\partial x}\bigg|_{x=L}$$

$K_{p_{elastelect_a}}$ and $K_{p_{elastelect_s}}$ in Eq. (8) are the matrices of the elastic-electric effect of the piezoelectric actuator and sensor layers, respectively.

$$K_{p_{elastelect_a}} \text{ or } K_{p_{elastelect_s}} = \begin{bmatrix} K_{pee_1} & K_{pee_2} & \cdots & K_{pee_N} \end{bmatrix} \tag{11}$$

where K_{pee_n} is the vector of the nth column of the elastic-electric matrix.

$$K_{pee_n} = \frac{e_{31_n}}{h_{p_n}} \int_{PZT_n} z \frac{\partial^2 s}{\partial x^2} d\mathrm{v} \tag{12}$$

$K_{p_{elect}}$ is a diagonal capacitance matrix of the piezoelectric patches.

$$K_{p_{elect}} = \sum_{n=1}^{N} \int_{PZT_n} \varepsilon_{p_n} p_n p_n^T dv \tag{13}$$

where the $N \times 1$ vector p_n has zero entries except for entry n which is equal to $1/h_{p_n}$.

Equation (8) can be rewritten as the following compact form

$$\begin{aligned} M\ddot{q} + Kq &= -K_{p_{elastelect_a}} v_a + f_d \\ v_s &= K^{-1}_{p_{elect}} K^T_{p_{elastelect_s}} q \end{aligned} \tag{14}$$

Herein

$$\begin{aligned} M &= M_b + M_p \\ K &= K_b + K_p + K_W \\ f_d &= -\ddot{y}_b \int_0^l \rho_b s dx - \ddot{y}_b \sum_N \int_{x_1}^{x_2} \rho_{p_n} s dx \end{aligned} \tag{15}$$

Equation (14) is the standard form of the governing equation of a dynamical system.

3 ROBUST LYAPUNOV BASED CONTROL

Since in this problem the effects of the support excitation appear as an external disturbances, so a robust Lyapunov based control is applied to suppress the flutter vibration of the beam. The controller voltages which are applied to the piezoelectric actuators can be defined as follows.

$$v_a = -K^+_{p_{elastelect\,a}} (M\ddot{\zeta} + Kq - K_D\lambda - \hat{f}_d) \tag{16}$$

Herein $\hat{f}_d$ is an estimate of f_d which is the disturbance term in Eq. (14) and the superscript $(+)$ denote the pseudo-inverse matrix. The parameters ζ and λ are defined as

$$\begin{aligned} \dot{\zeta} &= \dot{q}_d - A(\cdot)\tilde{q} \\ \lambda &= B^{-1}(\cdot)\tilde{q} \end{aligned} \tag{17}$$

Where q_d is the desired value of the generalized coordinate, q, and $\tilde{q} = q - q_d$. $A(\cdot)$ is a linear operator that should be chosen so that $B(\cdot)$ is strictly proper and stable. The relation between $A(s)$ and $B(s)$ is

$$B^{-1}(s) = sI + A(s) \tag{18}$$

The following error equation will be obtained by substituting Eq. (16) into Eq. (14).

$$M\dot{\lambda} + K_D\lambda = \tilde{f}_d \tag{19}$$

Where $\tilde{f}_d = f_d - \hat{f}_d$.
Now consider the following Lyapunov function

$$V = \frac{1}{2}\lambda^T M\lambda + \frac{1}{2}\tilde{f}_d^T K_I^{-1}\tilde{f}_d \tag{20}$$

Where K_I is a positive definite matrix. The time derivative of Eq. (20) is

$$\dot{V} = \lambda^T M\dot{\lambda} + \tilde{f}_d^T K_I^{-1}\dot{\tilde{f}}_d \tag{21}$$

Substituting the magnitude of the $M\dot{\lambda}$ from error equation (19), Eq. (21) can be rewritten as

$$\dot{V} = -\lambda^T K_D\lambda + \tilde{f}_d^T(\lambda - K_I^{-1}\dot{\hat{f}}_d) \tag{22}$$

To cancel the last term of Eq. (22), the following estimation law for $\hat{f}_d$ is defined.

$$\dot{\hat{f}}_d = K_I\lambda \tag{23}$$

So the time derivative of the Lyapunov function is determined as

$$\dot{V} = -\lambda^T K_D\lambda \tag{24}$$

Since the Lyapunov function, V, is positive definite and the time derivative of it, $\dot{V}$, is negative semi-definite, the states λ, and $\tilde{f}_d$ are bounded. Considering Eq. (19), it can be shown that if the mapping $-\lambda \to \tilde{f}_d$ is a passive mapping relative to V_1, namely

$$\int_0^t -\lambda(\tau)\tilde{f}_d(\tau)d\tau = V_1(t) - V_1(0) \quad for\,all\,t \geq 0 \tag{25}$$

then $\tilde{q} \in L_2 \cap L_\infty$, $\dot{\tilde{q}} \in L_2$, and $\tilde{q}$ is continuous and tends to zero asymptotically (Lewis et al., 1993). To show that $-\lambda \to \tilde{f}_d$ is a passive mapping, consider the following equation which can be obtained from Eq. (23)

$$-\lambda^T\tilde{f}_d = -\tilde{f}_d^T K_I^{-1}\dot{\tilde{f}}_d \tag{26}$$

Thus

$$-\int_0^t \lambda^T\tilde{f}_d d\tau = -\frac{1}{2}\int_0^t \frac{d}{d\tau}(\tilde{f}_d^T K_I^{-1}\tilde{f}_d) = \frac{1}{2}\tilde{f}_d^T(t)K_I^{-1}\tilde{f}_d(t) - \frac{1}{2}\tilde{f}_d^T(0)K_I^{-1}\tilde{f}_d(0) = V_1(t) - V_1(0) \tag{27}$$

So, the mapping $-\lambda \to \tilde{f}_d$ is a passive mapping relative to $V_1 = \frac{1}{2}\tilde{f}_d^T(t)K_I^{-1}\tilde{f}_d(t)$ and the convergency of the system is proved.

4 SIMULATION RESULTS AND CONCLUSIONS

In this section the simulation results are presented. Material properties of the beam and piezoelectric layers are illustrated in Table 1. The dimensionless parameters which are used in the numerical simulation are: $\overline{P} = \frac{P}{P_{cr}}$, $\overline{\omega} = \rho bh \frac{\omega^2 L^4}{EI}$, where $P_{cr} = \pi^2 EI / L^2$ is the Euler buckling load, and ω is the natural frequency of the beam.

Parameters	Value
Beam length	1 m
Beam wide	0.08 m
Beam high	0.02 m
Beam density	7000 kg/m3
Young modulus of Beam	200 GPa
Young modulus of PZT	61 GPa
Beam Moment of inertia	12.5 × 10-12 m4
PZT Moment of inertia	1.5 × 10-13 m4

Table 1: The magnitude of the system parameters.

Figure 2 compares the first two dimensionless natural frequencies of the beam with the results presented by Wang et al. (2002).

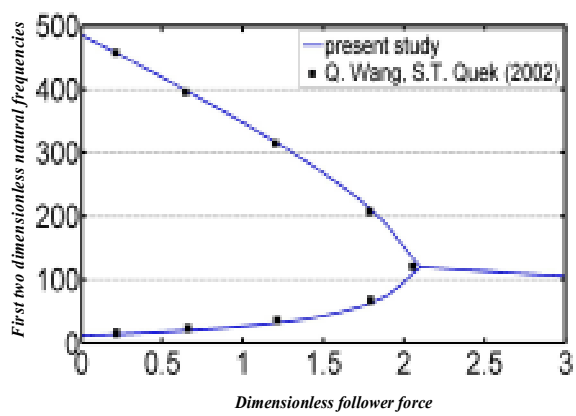

Figure 2: Validation of first two dimensionless natural frequencies versus dimensionless follower force.

This figure illustrates that if the magnitude of the dimensionless follower force is a little more than two, then the flutter instability happens. To simulate the system two cases are considered. The support excitation function is different in each case. Two types of functions are considered as support excitation; these functions are sinusoidal and square ones. To show the performance and capability of the controller, in all simulations the controller gains are same and are $K_D = 500\,I$ and

$K_I = 20I$. Where I is an identity matrix. In each case the effect of the three different values of the follower forces are studied. To control the vibrations of the beam three pair of piezoelectric layers are considered to be attached to the both side of the beam. The length of these piezoelectric layers for all cases is 0.1m. Figure 3 shows the tip vibration of the beam while a sinusoidal support excitation is applied to it and subjected to a follower force with magnitude $\overline{P} = 0.5$.

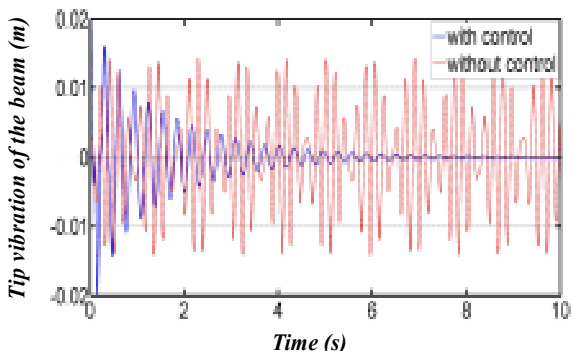

Figure 3: Time response of the tip vibration of the beam when sinusoidal support excitation is applied ($\overline{P} = 0.5$)

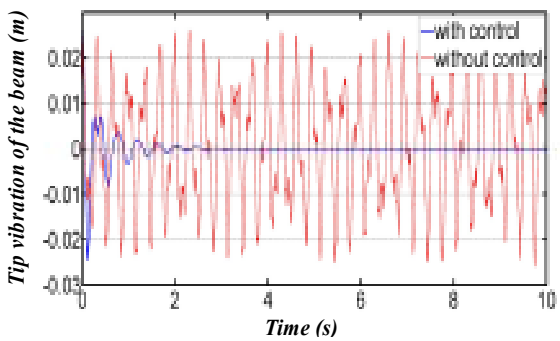

Figure 4: Time response of the tip vibration of the beam when sinusoidal support excitation is applied ($\overline{P} = 1$)

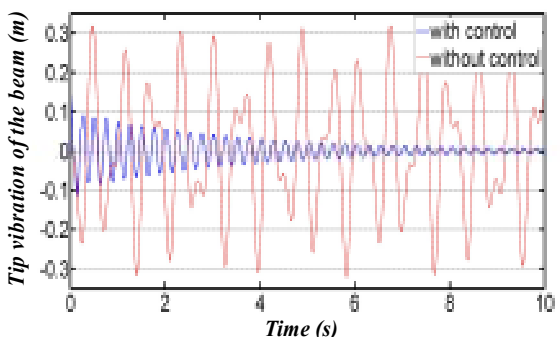

Figure 5: Time response of the tip vibration of the beam when sinusoidal support excitation is applied ($\overline{P} = 2$)

This figure shows the effectiveness of the robust controller and illustrates how the piezoelectric actuators damp the vibration of the beam. Figure 4 and 5 show the tip vibration of the sinusoidal support excited beam when $\overline{P}=1$, and $\overline{P}=2$, respectively. It is illustrated that when the magnitude of the dimensionless follower force is close to the instability condition the amplitude of the vibrations increased several times; it is noteworthy to say that, the flutter vibrations of the beam is suppressed in this condition, too. Figure 6-8 present the tip vibration of the beam in which a square support excitation is applied to the system.

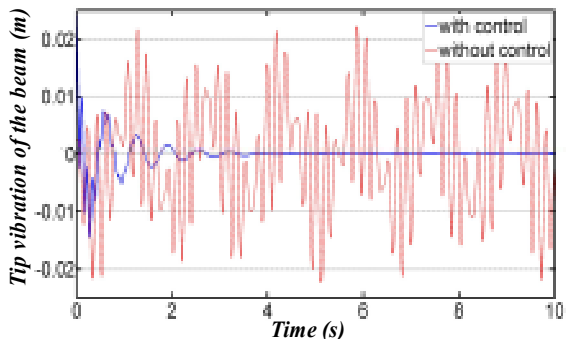

Figure 6: Time response of the tip vibration of the beam when square support excitation is applied ($\overline{P}=0.5$).

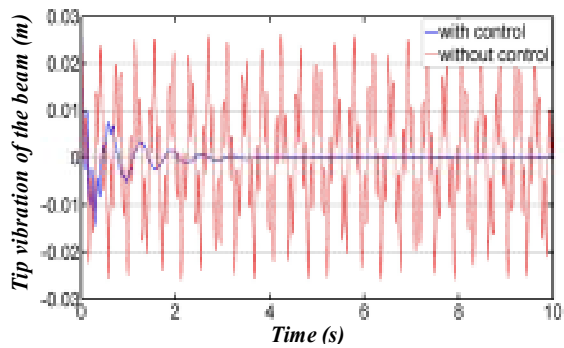

Figure 7: Time response of the tip vibration of the beam when square support excitation is applied ($\overline{P}=1$).

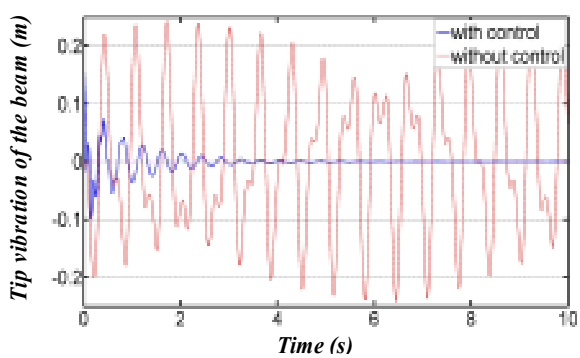

Figure 8: Time response of the tip vibration of the beam when square support excitation is applied ($\overline{P}=2$).

The effects of variation of the magnitude of the follower force are illustrated in these figures. The actuator voltages when the beam subjected to a sinusoidal support excitation and $\overline{P}=1$ are shown in Fig. (9). This figure illustrates that these voltages are in admissible limits.

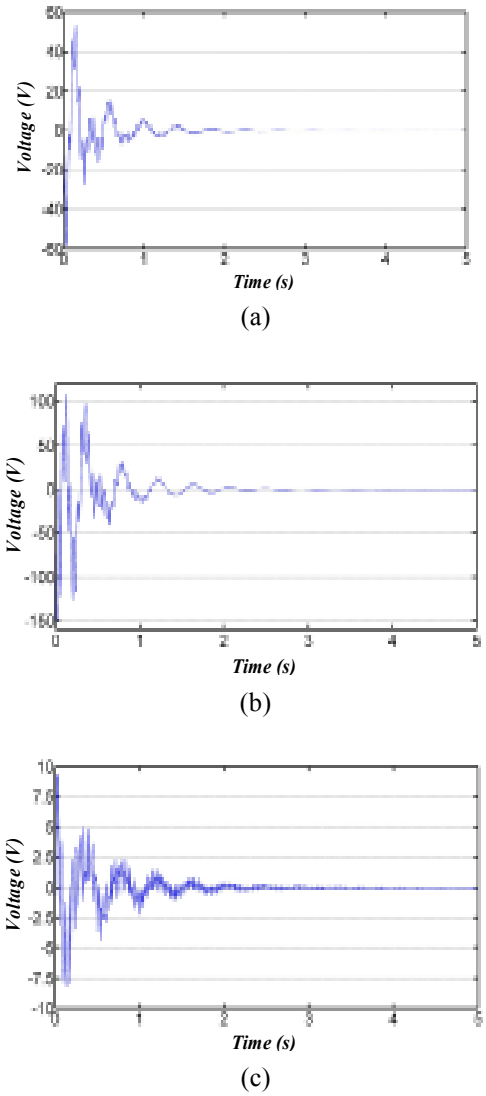

Figure 9: The applied voltages to the actuators. (a) first piezoelectric layer, (b) second piezoelectric layer, (c) third piezoelectric layer. (sinusoidal support excitation, and $\overline{P}=1$).

To illustrate the capability of the controller scheme, the effects of the parameter uncertainties and instrument disturbances are studied when the beam is excited by a sinusoidal function and $\overline{P}=1$. Figure (10) shows the effects of the %10, and %20 uncertainties of the f_d in the beam vibrations. The effects of the %10, %15, and %25 instrument disturbances are shown in Fig. (11).

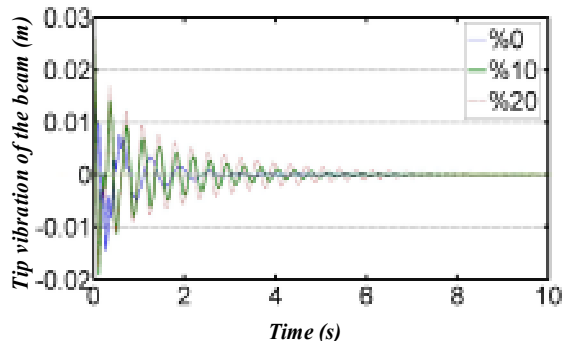

Figure 10: Time response of the tip vibration of the beam by considering %0, %10, and %20 parameter uncertainty (sinusoidal support excitation and $\overline{P}=1$).

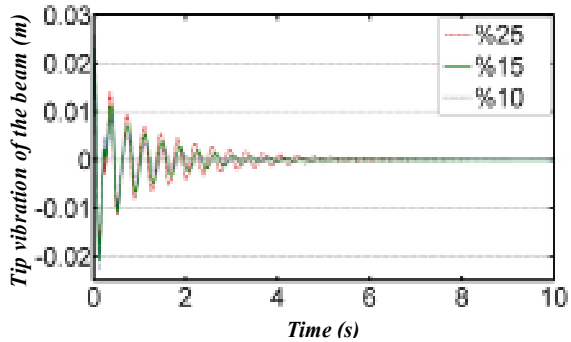

Figure 11: Time response of the tip vibration of the beam by considering %10, %15, and %25 instrument disturbances (sinusoidal support excitation and $\overline{P}=1$).

Figure (12) shows the tip vibration of the beam by considering %10 instrument disturbances and %10 parameter uncertainty. These last three figures illustrate that although by increasing the parameter uncertainties and instrument disturbances the amplitude of the controlled vibrations increased, but these vibrations are damped in few seconds, too. These simulation results show the effectiveness and robustness of the controller.

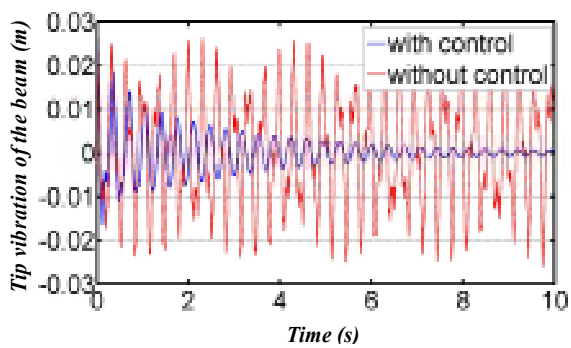

Figure 12: Time response of the tip vibration of the beam by considering %10 instrument disturbances and %10 parameter uncertainty (sinusoidal support excitation and $\overline{P}=1$).

References

Alhazza, K. A., Nayfeh, A. H., Daqaq, M. F. (2009). On utilizing delayed feedback for active-multimode vibration control of cantilever beams. Journal of Sound and Vibration 319(3): 735-752.

Azadi, V., Azadi, M., Fazelzadeh, S. A., Azadi, E. (2014). Active control of an FGM beam under follower force with piezoelectric sensors/actuators. International Journal of Structural Stability and Dynamics14(3): 1350063-1-19.

Fazelzadeh, S. A., Eghtesad, M., Azadi, M. (2010). Buckling and flutter of a column enhanced by piezoelectric layers and lumped mass under a follower force. International Journal of Structural Stability and Dynamics 10(5): 1083-1097.

Fazelzadeh, S. A., Kazemi-Lari, M. A. (2013). Stability analysis of partially loaded Leipholz column carrying a lumped mass and resting on elastic foundation. Journal of Sound and Vibration 332(3): 595-607.

Foutsitzi, G., Marinova, D. G., Hadjigeorgiou, E., & Stavroulakis, G. E. (2003, August). Robust H_2 vibration control of beams with piezoelectric sensors and actuators. In Physics and Control, International Conference on (Vol. 1, pp. 157-162). IEEE.

Jalili, N., Dadfarnia, M., Hong, F., & Ge, S. S. (2002). Adaptive non model-based piezoelectric control of flexible beams with translational base. In American Control Conference, 2002. Proceedings of the 2002 (Vol. 5, pp. 3802-3807). IEEE.

Ji, H., Qiu, J., Zhu, K., Badel, A. (2010). Two-mode vibration control of a beam using nonlinear synchronized switching damping based on the maximization of converted energy. Journal of Sound and Vibration 329(14): 2751-2767.

Kucuk, I., Sadek, I., Yilmaz, Y. (2014). Optimal control of a distributed parameter system with applications to beam vibrations using piezoelectric actuators. Journal of the Franklin Institute 351(2): 656-666.

Kucuk, I., Sadek, I. S., Zeini, E., Adali, S. (2011). Optimal vibration control of piezolaminated smart beams by the maximum principle. Computers & Structures 89(9): 744-749.

Kuo, C. F. J., Tu, H. M., Huy, V. Q., Liu, C. H. (2013). Dynamic stability analysis and vibration control of a rotating elastic beam connected with an end mass. International Journal of Structural Stability and Dynamics 13(03).

Lewis, F. L., Abdallah,C. T., Dawson, D. M. (1993). Control of robot manipulators. Vol. 866. Macmillan Publishing Company.

Lin, J., Liu, W. Z. (2006). Experimental evaluation of a piezoelectric vibration absorber using a simplified fuzzy controller in a cantilever beam. Journal of sound and vibration 296(3): 567-582.

Lin, J. C., Nien, M. H. (2005). Adaptive control of a composite cantilever beam with piezoelectric damping-modal actuators/sensors. Composite structures 70(2): 170-176.

Mahmoodi, S. N., Jalili, N., Khadem, S. E. (2008). An experimental investigation of nonlinear vibration and frequency response analysis of cantilever viscoelastic beams. Journal of Sound and vibration 311(3): 1409-1419.

Prokic, A., Besevic, M., Lukic, D. (2014). A numerical method for free vibration analysis of beams. Latin American Journal of Solids and Structures 11: 1432-1444.

Santillan, S. T., Plaut, R. H., Witelski, T. P., Virgin, L. N. (2008). Large oscillations of beams and columns including self-weight. International Journal of Non-Linear Mechanics 43(8): 761-771.

Sinir, B. G., Ozhan, B. B., Reddy, J. N. (2014). Buckling configurations and dynamic response of buckled Euler-Bernoulli beams with non-classical supports. Latin American Journal of Solids and Structures 11: 2516-2536.

Sun, D., Mills, J. K., Shan, J., Tso, S. K. (2004). A PZT actuator control of a single-link flexible manipulator based on linear velocity feedback and actuator placement. Mechatronics 14(4): 381-401.

Trindade, M. A. (2011). Experimental analysis of active-passive vibration control using viscoelastic materials and extension and shear piezoelectric actuators. Journal of Vibration and Control: 17(6), 917-929.

Wang, L., Chen, H., He, X. (2011). Active H_∞ control of the vibration of an axially moving cantilever beam by magnetic force. Mechanical Systems and Signal Processing 25(8): 2863-2878.

Wang, Q.,Quek, S. T. (2002). Enhancing flutter and buckling capacity of column by piezoelectric layers. International Journal of Solids and Structures 39: 4167-4180.

Xinke, G., & Haimin, T. (2007, August). Active vibration control of a cantilever beam using bonded piezoelectric sensors and actuators. In Electronic Measurement and Instruments, 2007. ICEMI'07. 8th International Conference on (pp. 4-85). IEEE.

Youssef, H. M., El-Bary, A. A., Elsibai, K. A., (2014). Vibration of Gold Nano Beam in Context of Two-Temperature Generalized Thermoelasticity Subjected to Laser Pulse. Latin American Journal of Solids and Structures 12: 37-59.